Electronic Supplementary Material (ESI) for Journal of Materials Chemistry A.
This journal is © The Royal Society of Chemistry 2022

Supplementary Information

Heterogeneous doping of visible-light-responsive $Y_2Ti_2O_5S_2$ for enhanced hydrogen evolution

Hiroaki Yoshida[1, 2], Zhenhua Pan[3], Ryota Shoji[4], Vikas Nandal[5], Hiroyuki Matsuzaki[4], Kazuhiko Seki[5], Takashi Hisatomi[3], and Kazunari Domen[3, 6*]

[1] Mitsubishi Chemical Corporation, Science & Innovation Center, 1000 Kamoshida-cho, Aoba-ku, Yokohama-shi, Kanagawa 227-8502, Japan

[2] Japan Technological Research Association of Artificial Photosynthetic Chemical Process (ARPChem), Tokyo, Japan

[3] Research Initiative for Supra-Materials, Shinshu University, 4-17-1 Wakasato, Nagano-shi, Nagano 380-8553, Japan

[4] Research Institute for Material and Chemical Measurement, National Metrology Institute of Japan (NMIJ), National Institute of Advanced Industrial Science and Technology (AIST), Tsukuba 1-1-1 Higashi, Tsukuba, Ibaraki 305-8565, Japan.

[5] Global Zero Emission Research Center, National Institute of Advanced Industrial Science and Technology, Tsukuba 16-1 Onogawa, Ibaraki 305-8569, Japan

[6] Office of University Professors, The University of Tokyo, 2-11-16 Yayoi, Bunkyo-ku, Tokyo 113-8656, Japan

*Corresponding email address: domen@chemsys.t.u-tokyo.ac.jp; domen@shinshu-u.ac.jp

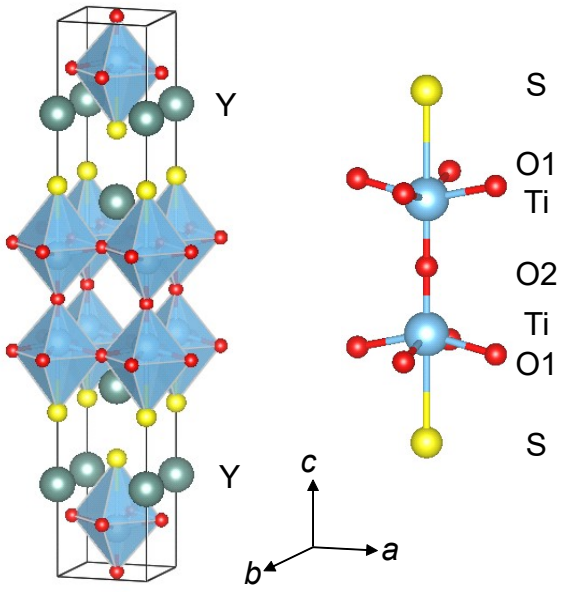

Figure S1 A schematic illustration for the crystal structure of $Y_2Ti_2O_5S_2$.[1]

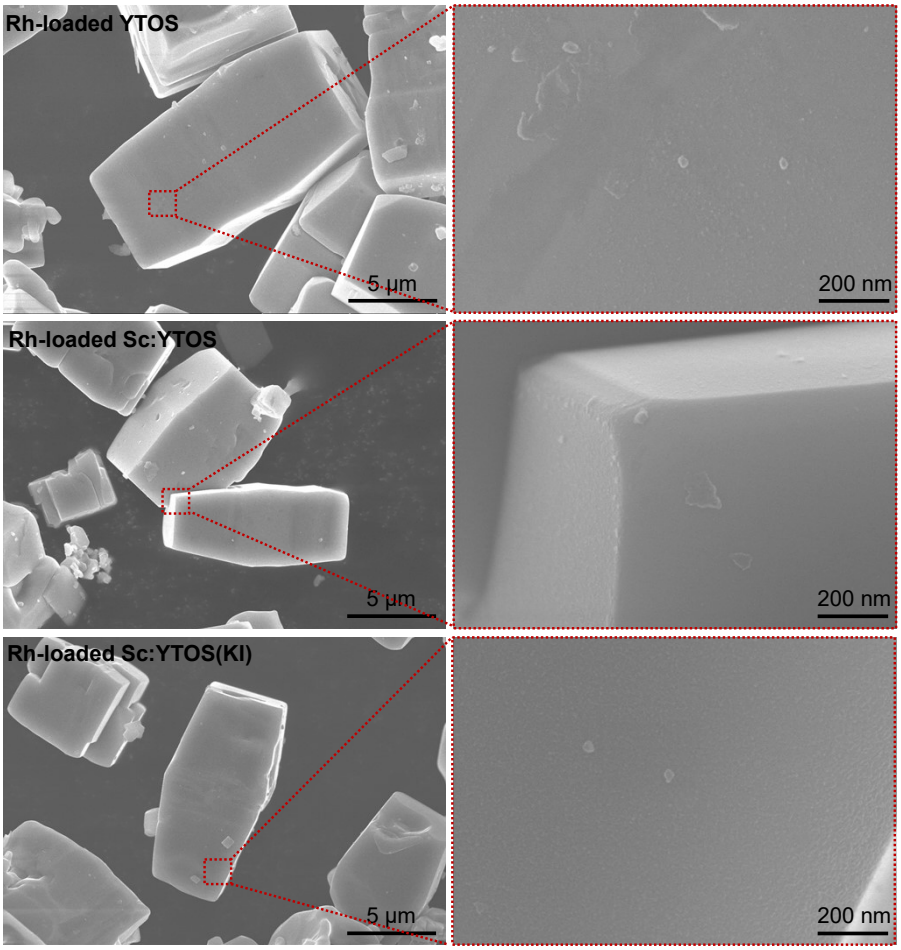

Figure S2 SEM images of Rh-loaded YTOS, Rh-loaded Sc:YTOS and Rh-loaded Sc:YTOS(KI).

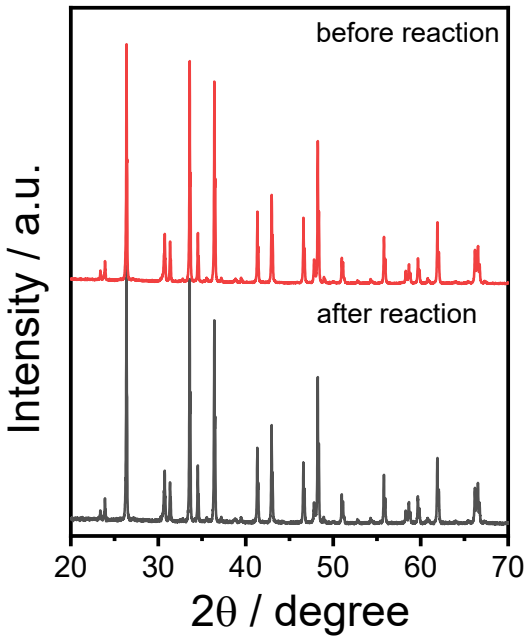

Figure S3 XRD patterns for Rh-loaded Sc:YTOS(KI)-ac before and after photocatalytic H_2 evolution.

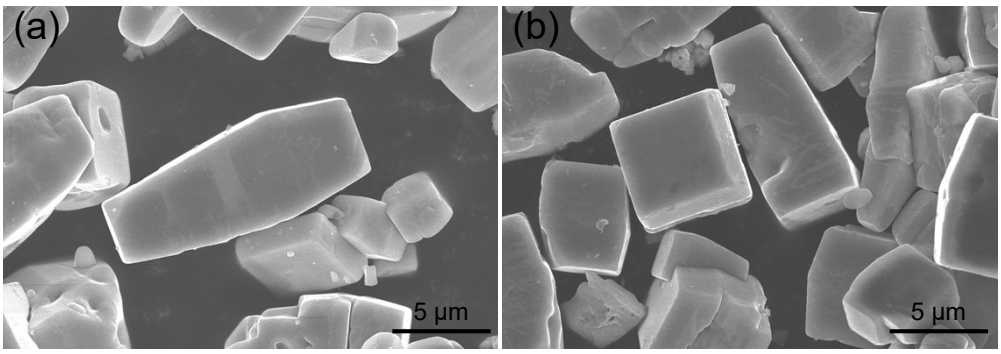

Figure S4 SEM images for Rh-loaded Sc:YTOS(KI)-ac (a) before and (b) after photocatalytic H_2 evolution.

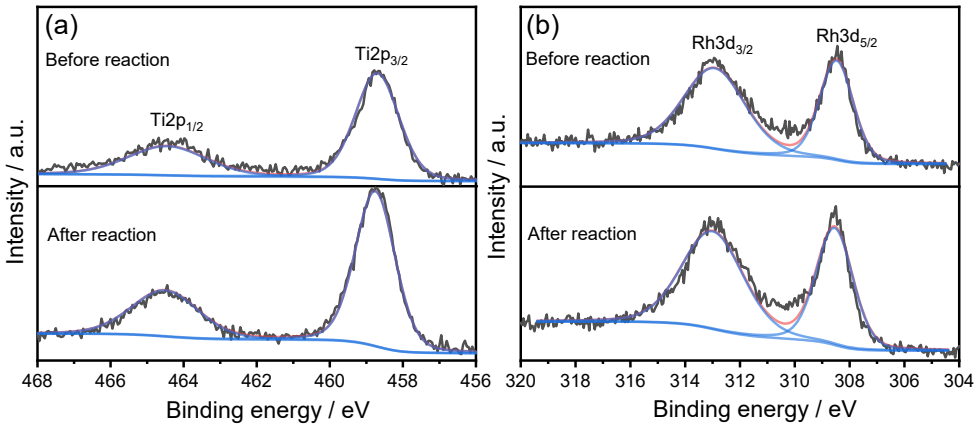

Figure S5 (a) Ti 2*p* and (b) Rh 3*d* XPS spectra obtained from Rh-loaded Sc:YTOS(KI)-ac before and after photocatalytic H_2 evolution.

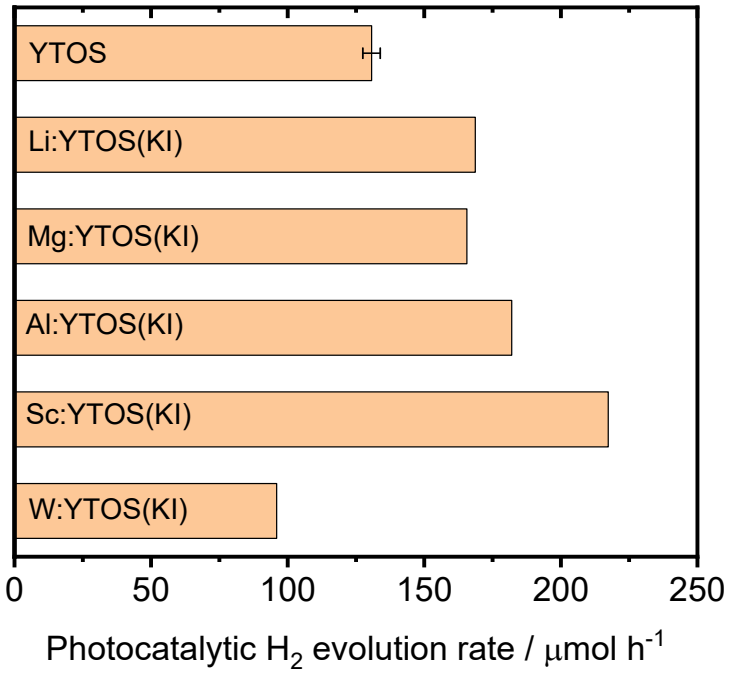

Figure S6 Photocatalytic H_2 evolution activities of YTOS and Me:YTOS(KI). Me = Li, Mg, Al Sc, and W. Reaction conditions: photocatalyst amount, 0.3 g; cocatalyst, Rh 2 wt% loaded by photodeposition; reactant solution, 150 mL (20 mM Na_2S + 20 mM Na_2SO_3) aqueous solution; background atmosphere, water vapor and 50 torr Ar; light source, a 300 W Xe lamp with a cut-off filter (λ > 420 nm). The error bar of YTOS was obtained by repeating the measurement for 3 times.

Table S1 Molar ratios of YTOS, Sc:YTOS(KI) and Sc:YTOS(KI)-ac determined by ICP-AES.

Sample	Sc/Ti
YTOS	< 0
YTOS:Sc(KI)	0.8%
YTOS:Sc(KI)-ac	0.6%

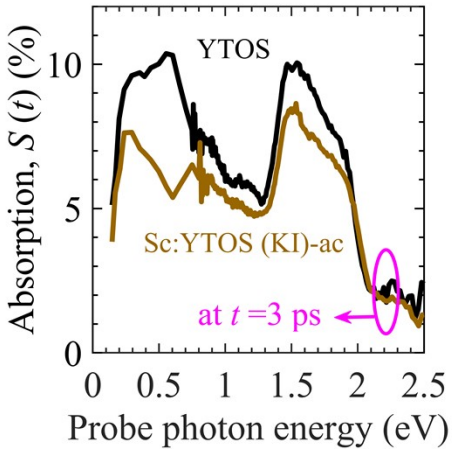

Figure S7. TDR spectra for YTOS and Sc:YTOS(KI)-ac at pump fluence intensity P_{FL} = 3 μJ per pulse and time t = 3 ps.

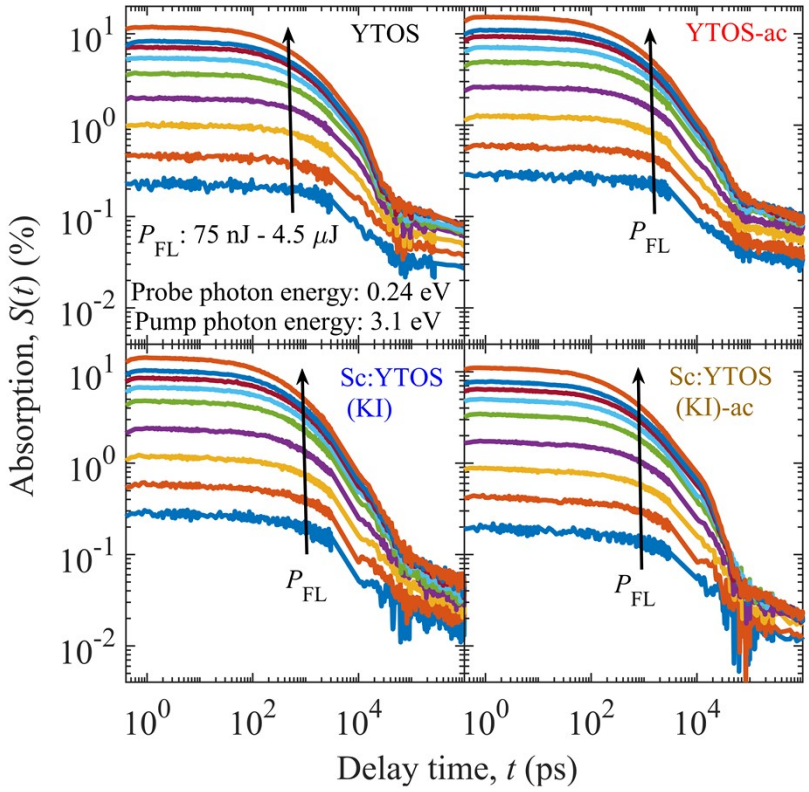

Figure S8. TDRS measurements of YTOS photocatalysts. Decay kinetics of TDR signal $S(t)$ with time t of YTOS, YTOS-ac, Sc:YTOS(KI), and Sc:YTOS(KI)-ac photocatalysts. The pump photon energy of 3.1 eV was employed to generate charge carriers. The density of generated charge carriers was changed by varying pump fluence intensity P_{FL} from 75 nJ per pulse to 4.5 μJ per pulse (0.075, 0.15, 0.2, 0.6, 1.2, 1.8, 2.4, 3.0, and 4.5 μJ). Arrow direction represents the increase of P_{FL}. The relaxation of these charge carriers was measured by probe photon energy of 0.24 eV.

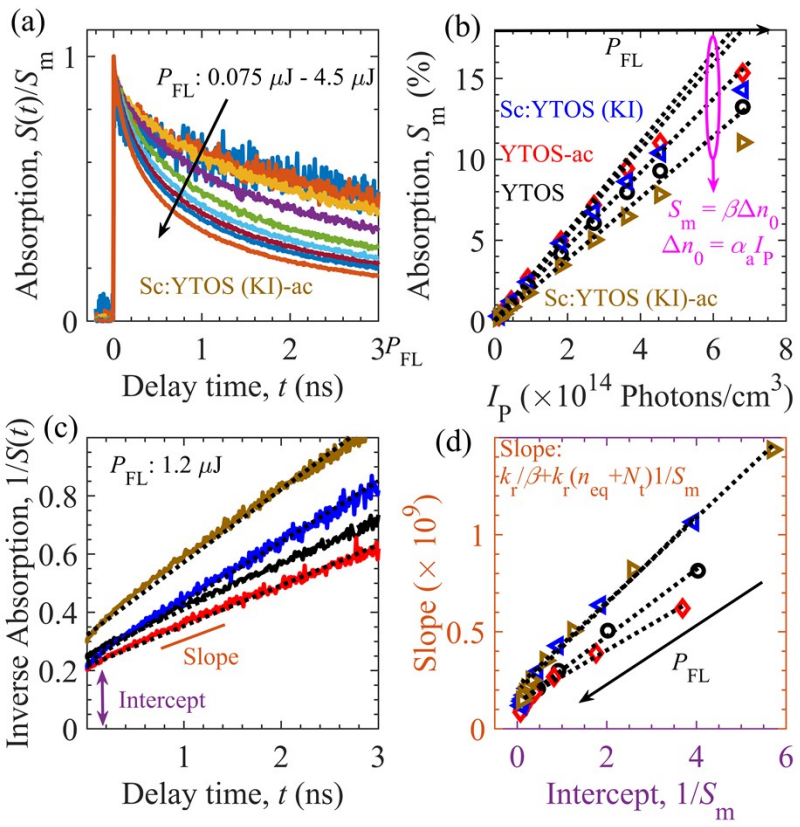

Figure S9. Early-time decay analysis of TDR signal of YTOS photocatalysts. (a) Normalized TDR signal $S(t)/S_m$ decay of Sc:YTOS(KI) photocatalyst in early ns time range at various pump fluence intensity P_{FL} ranging from 0.075 μJ per pulse to 4.5 μJ per pulse. (b) Increase in maximum absorption signal S_m (at $t \sim 1$ ps) with the increase of P_{FL}. Dotted lines are the linear fits (such that $S_m = \beta\Delta n_0$) to the measured data in low P_{FL} and pump photon density I_P range. Here, β is the proportionality constant and Δn_0 (= $\alpha_a I_p$; α_a is the absorption coefficient) is the initial photogenerated charge carrier density. (c) Inverse TDR signal $1/S(t)$ variation against t at P_{FL} = 1.2 μJ per pulse. (d) Slope versus intercept $1/S_m$ plots. Here, the symbols are the estimated slope and intercept of the linear fit (dotted line) to the measured data in panel (c). In panel (a) and (c), the increase of P_{FL} is represented by the arrow direction. The color scheme in panel (b-c) corresponds to respective photocatalysts. Since slope = $k_r/\beta + k_r(n_{eq} + N_t)1/S_m$, the initial guess of recombination rate constant k_r and sum of equilibrium electron density and trap density (*i.e.*, n_{eq} + N_t) are obtained from the linear fit (dotted line) in low P_{FL} range.

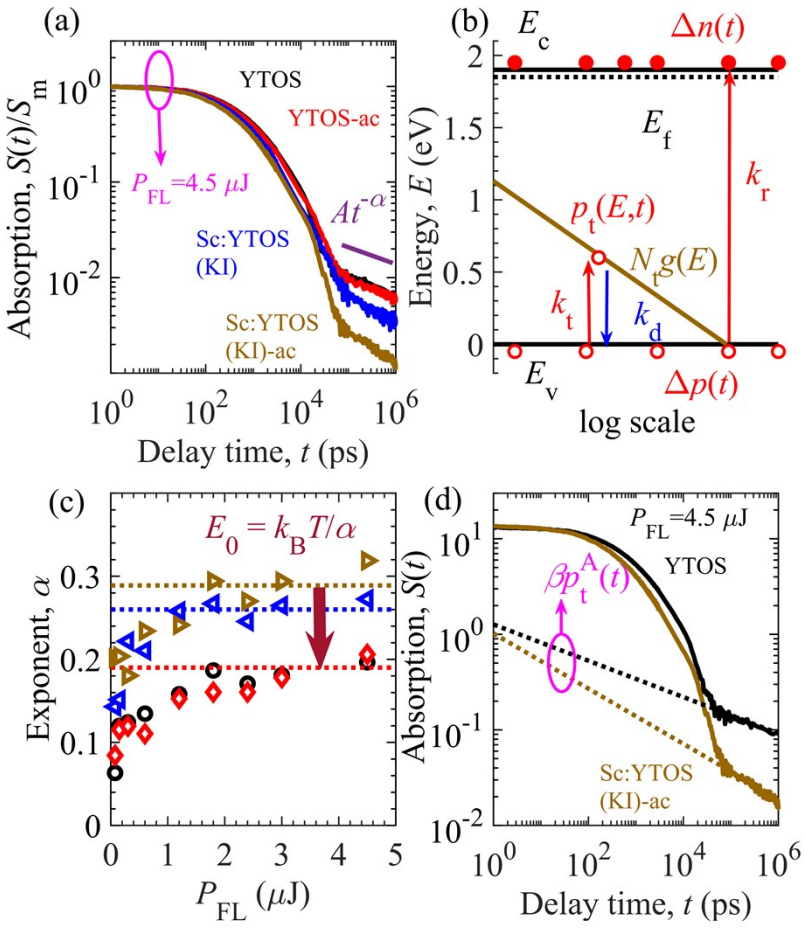

Figure S10. Late-time decay analysis of TDR signal of YTOS photocatalysts. (a) Normalized decay kinetics $S(t)/S_m$ decay characteristics of photocatalysts with time t at pump fluence intensity P_{FL} = 4.5 μJ per pulse. Here, S_m is maximum absorption signal at t ~ 1 ps and $S(t)$ follows power-law ($At^{-\alpha}$) decay features in late μs time range (~ 0.1 μs to 1 μs). (b) Proposed theoretical model highlighting dominant relaxation processes (bimolecular recombination, hole trapping, and detrapping) of charge carriers. The details are provided in Material and Methods section. (c) Exponent α at various P_{FL}. The characteristic energy $E_0 = k_B T/\alpha$ of exponential tail trap states (shown in panel (b)) of VB is reduced from 137 meV to 90-100 meV with Sc doping of YTOS photocatalyst. (d) Calibration of analytical model of trapped hole density p_t^A (dotted lines) to the measured data (solid line curves) in late μs time range. The detailed derivation of p_t^A is reported previously.[2] The analysis of absorption signal in late μs time range deduces initial guess for trap density, doping density, and characteristic energy of different photocatalysts.

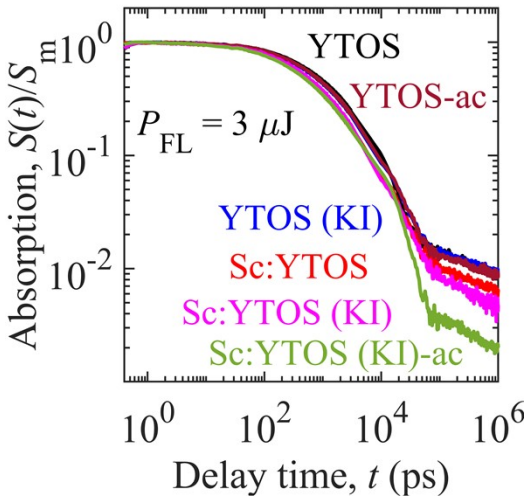

Figure S11. Normalized decay kinetics of TDR signal with time t of YTOS, YTOS-ac, YTOS(KI), Sc:YTOS, Sc:YTOS (KI), and Sc:YTOS (KI)-ac photocatalysts at pump fluence intensity P_{FL} = 3 μJ per pulse. Here, S_m is the maximum absorption signal at t ~ 1 ps.

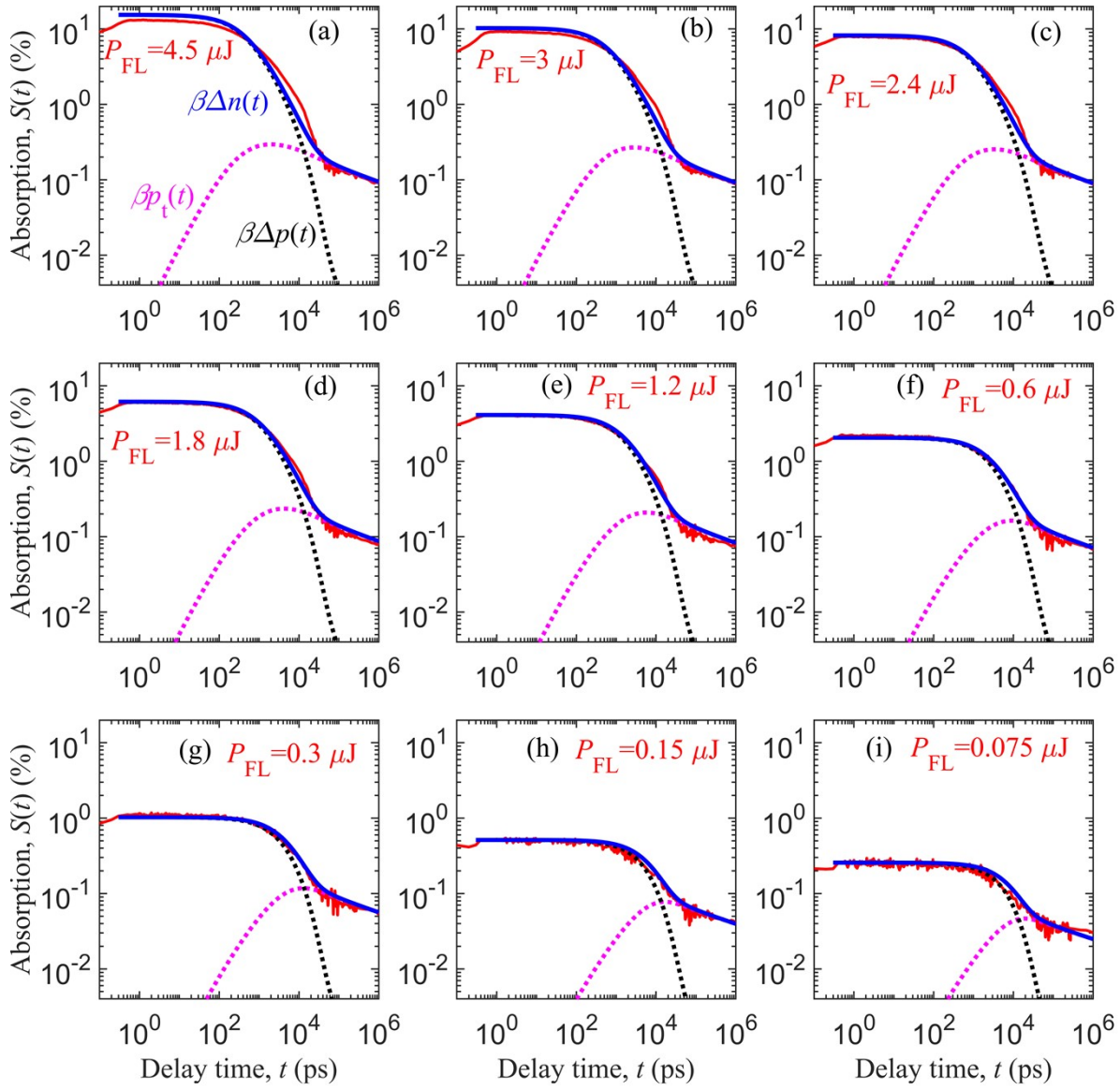

Figure S12. Charge carrier dynamics of YTOS photocatalyst under various pump fluence intensity P_{FL} ranging from 0.075 μJ per pulse to 4.5 μJ per pulse. The photocatalyst was prepared by solid state reaction (SSR) method. The red solid, blue solid, pink dotted, and black dotted line curves correspond to measured absorption signal $S(t)$, excess density of mobile electrons $\Delta n(t)$, trapped holes, and mobile holes $\Delta p(t)$, respectively. The simulation results agree with the measurements.

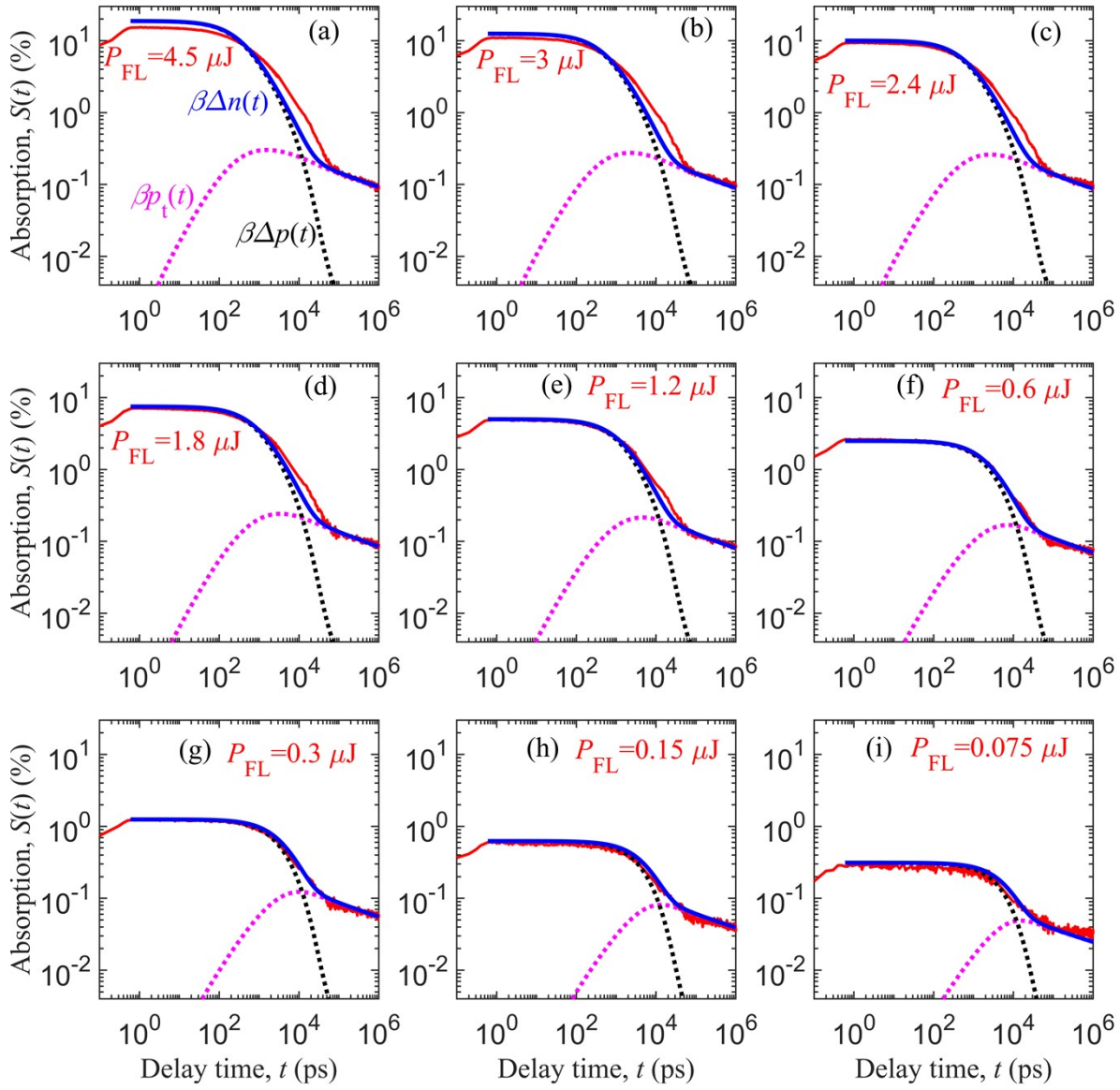

Figure S13. Charge carrier dynamics of YTOS-ac photocatalyst for different pump fluence intensity P_{FL} varying from 0.075 μJ per pulse to 4.5 μJ per pulse. The photocatalyst was prepared by solid state reaction and following acid treatment methods. The red solid, blue solid, pink dotted, and black dotted line curves correspond to measured data, mobile electron density $\Delta n(t)$, trapped hole density p_t(t), and mobile hole density $\Delta p(t)$, respectively. The simulation results corroborate well with the measurements.

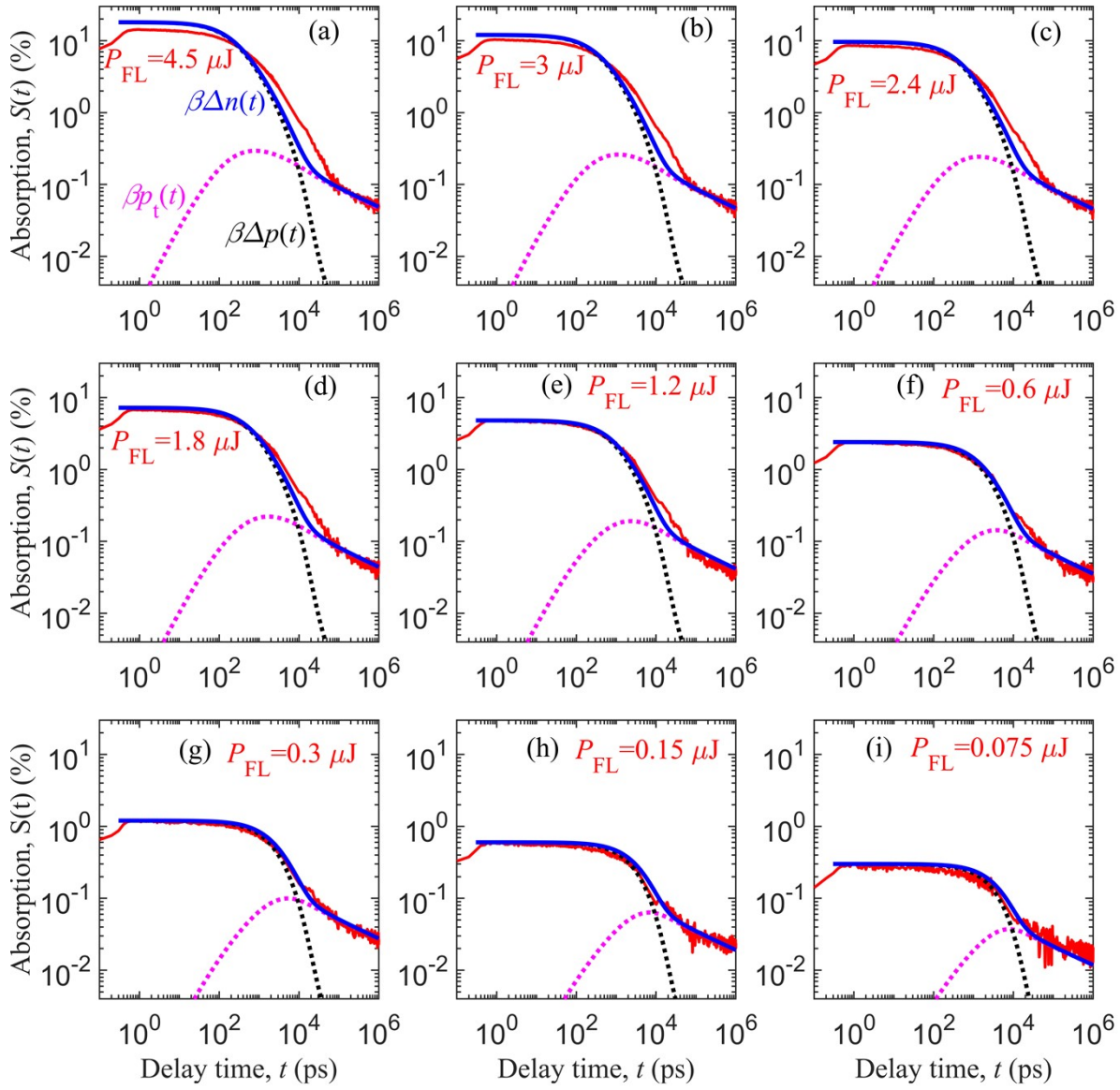

Figure S14. Charge carrier dynamics of Sc:YTOS(KI) photocatalyst at several pump fluence intensity P_{FL} varying from 0.075 μJ per pulse to 4.5 μJ per pulse. The photocatalyst was prepared by KI flux method. Here, the red solid, blue solid, pink dotted, and black dotted line curves correspond to measured data, mobile electron density $\Delta n(t)$, trapped hole density p_t(t), and mobile hole density $\Delta p(t)$, respectively. The simulation results reasonably match with the measured data.

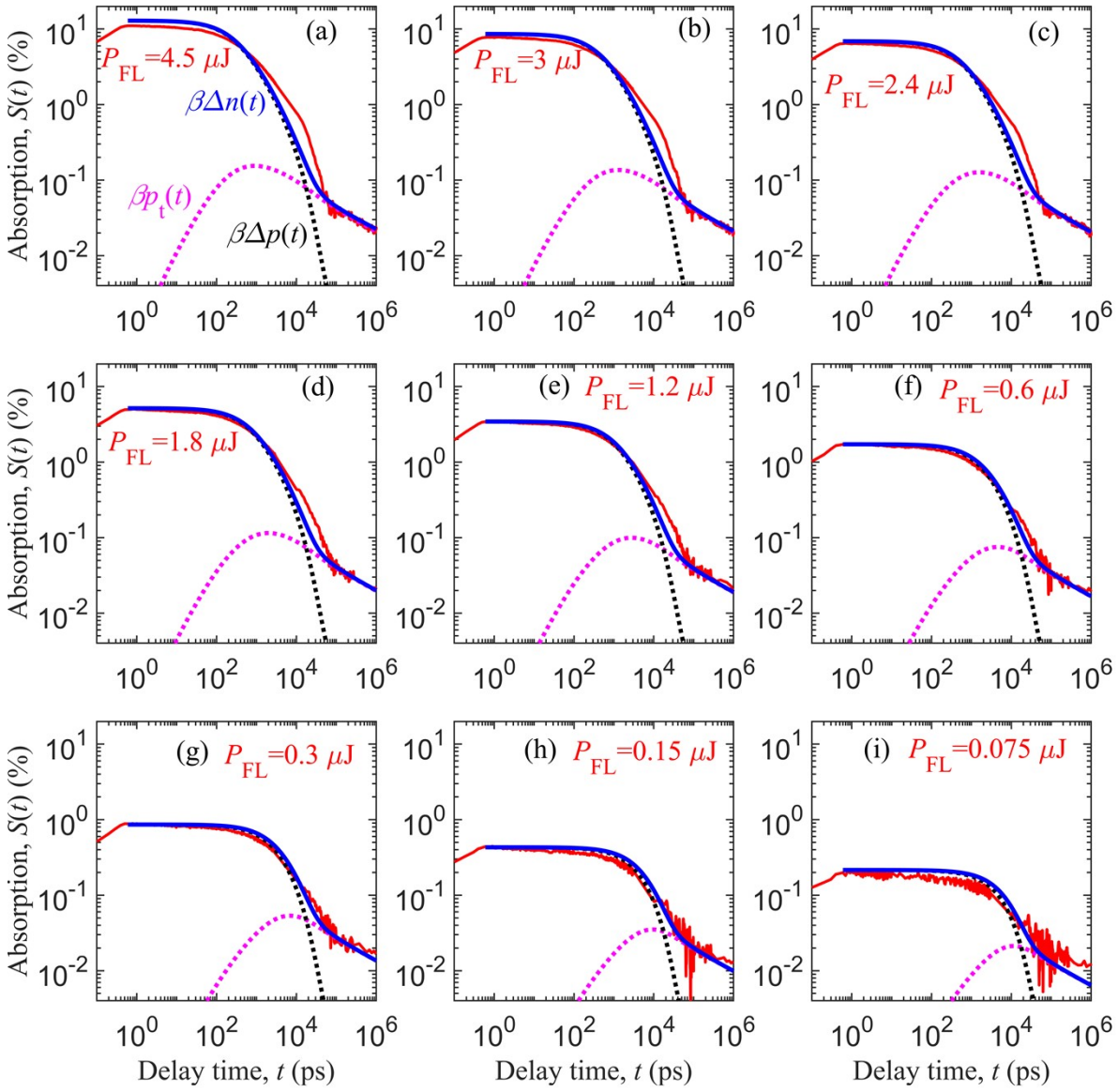

Figure S15. Charge carrier dynamics of Sc:YTOS(KI)-ac photocatalyst at several pump fluence intensity P_{FL} varying from 0.075 μJ per pulse to 4.5 μJ per pulse. The photocatalyst was prepared by KI flux method and acid treatment. Here, the red solid, blue solid, pink dotted, and black dotted line curves correspond to measured data, mobile electron density $\Delta n(t)$, trapped hole density $p_t(t)$, and mobile hole density $\Delta p(t)$, respectively. The simulation results are calibrated to the measured data.

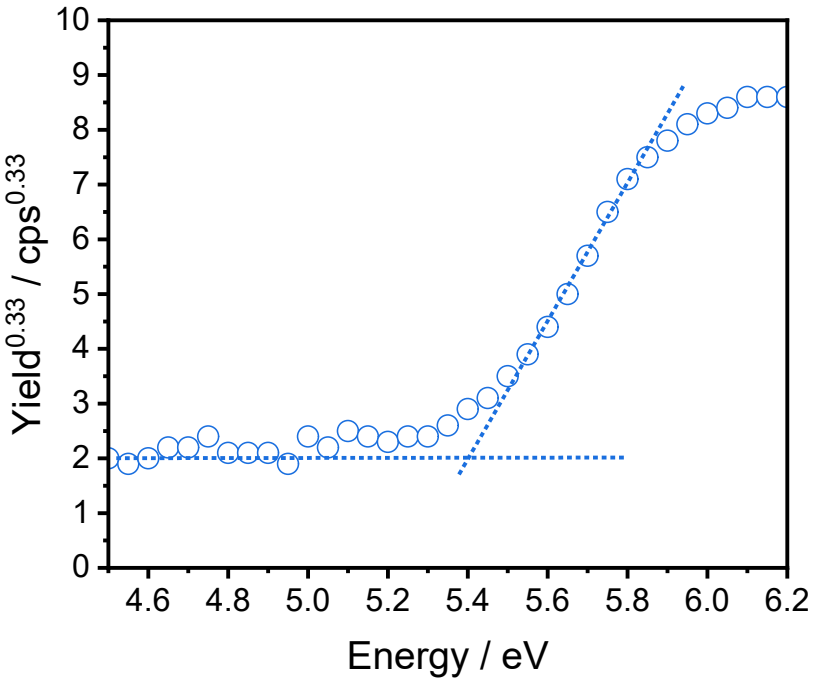

Figure S16 PESA spectrum of Sc:$Y_2Ti_2O_5S_2$(KI)-ac. The valence band maximum was 5.4 eV vs. vacuum.

Table S2. Evaluated material parameters from the theoretical analysis of absorption signal $S(t)$ decay features of various YTOS photocatalysts.

Parameters, symbols (units)	YTOS	YTOS-ac	Sc:YTOS(KI)	Sc:YTOS(KI)-ac
Effective density of states of VB, N_v (cm^{-3})	10^{20} (ref [2])	10^{20}	10^{20}	10^{20}
Absorption coefficient, α_a (cm^{-1}) at pump photon energy of 3.1 eV	17400 (ref [2])	17400	17400	17400
Charge carrier density at P_{FL} = 3μJ, Δn_0 (cm^{-3})	7.9×10^{20}	7.9×10^{20}	7.9×10^{20}	7.9×10^{20}
Proportionality constant,	1.30×10^{18}	1.58×10^{18}	1.52×10^{18}	1.09×10^{18}

β (cm^3)				
Recombination/trapping rate constant, $k_{r,t}$ (cm^3 s^{-1})	1.70×10^{-10}	2.16×10^{-10}	2.94×10^{-10}	2.36×10^{-10}
Equilibrium electron density, n_{eq} (cm^{-3})	5×10^{17}	5×10^{17}	6×10^{17}	4×10^{17}
Characteristic energy of VB tail state, E_0 (meV)	137	137	100	90
Trap density of VB tail state, N_t (cm^{-3})	5.1×10^{17}	4.3×10^{17}	5.2×10^{17}	4×10^{17}

After the fine-tunning, the evaluated material parameters ($k_{r,t}$ and n_{eq}) of YTOS are slightly different from the previously reported values.[2] ($k_{r,t}$ changes from 1.57×10^{-10} cm^3 s^{-1} to 1.70×10^{-10} cm^3 s^{-1}, and n_{eq} changes from 5.2×10^{17} cm^{-3} to 5×10^{17} cm^{-3}.)

Reference

1. A. Ishikawa, T. Takata, T. Matsumura, J. N. Kondo, M. Hara, H. Kobayashi and K. Domen, *J. Phys. Chem. B*, 2004, **108**, 2637-2642.
2. V. Nandal, R. Shoji, H. Matsuzaki, A. Furube, L. Lin, T. Hisatomi, M. Kaneko, K. Yamashita, K. Domen and K. Seki, *Nat. Commun.*, 2021, **12**, 7055.